Published in final edited form as:
Nat Immunol. 2008 August ; 9(8): 908–916. doi:10.1038/ni.1634.

Autophagic control of *Listeria* through intracellular innate immune recognition in drosophila

Tamaki Yano[1], **Shizuka Mita**[1], **Hiroko Ohmori**[2], **Yoshiteru Oshima**[1], **Yukari Fujimoto**[3], **Ryu Ueda**[4], **Haruhiko Takada**[5], **William E. Goldman**[6], **Koichi Fukase**[3], **Neal Silverman**[7], **Tamotsu Yoshimori**[2], and **Shoichiro Kurata**[1*]

1*Graduate School of Pharmaceutical Sciences, Tohoku University, Sendai 980-8578, Japan*

2*Research Institute for Microbial Diseases, Osaka University, Osaka 565-0871, Japan, CREST, Japan Science and Technology Agency, Tokyo 103-0027, Japan*

3*Graduate School of Science, Osaka University, Osaka 560-0043, Japan*

4*National Institute of Genetics, Mishima, 411-8540, Japan*

5*Graduate School of Dentistry, Tohoku University, Sendai 980-8575, Japan*

6*Washington University School of Medicine, St. Louis, Missouri 63110, USA*

7*Department of Medicine, University of Massachusetts Medical School, Worcester, MA 01605, USA*

Abstract

Autophagy, an evolutionally conserved homeostatic process for catabolizing cytoplasmic components, has been implicated in the elimination of intracellular pathogens during mammalian innate immune responses. However, the mechanisms underlying cytoplasmic infection-induced autophagy, and the role of autophagy in host survival against intracellular pathogens are unknown. Here we report that in drosophila, recognition of diaminopimelic acid-type peptidoglycans by the pattern recognition receptor PGRP-LE is crucial for the induction of autophagy, and that autophagy prevents the intracellular growth of *Listeria monocytogenes* and promotes host survival against this infection. Autophagy induction occurs independently of the Toll and IMD innate signaling pathways. These findings define a clear pathway leading from the intracellular pattern recognition receptors to the induction of autophagy to host defense.

INTRODUCTION

The innate immune system is a powerful and evolutionally well-conserved barrier to infectious pathogens. In drosophila, which rely almost entirely on innate immunity to fight microbial infection, members of the peptidoglycan recognition protein (PGRP) family act as microbe sensors[1, 2]. These receptors are found in the hemolymph, on immune cell surfaces, and within the immune cells, and they recognize bacterial peptidoglycans and activate immune signaling pathways such as the Toll and IMD pathways. The Toll and IMD pathways control the production of antimicrobial peptides (AMPs) through NF-κB transcription factors[1,2]. PGRP-LE, a drosophila PGRP family member present both in the hemolymph and inside immune

Correspondence should be addressed to S.K. (kurata@mail.pharm.tohoku.ac.jp).

cells[3], binds to diaminopimelic acid (DAP)-type peptidoglycans (PGN)[4] and is sufficient for the induction of AMP genes following immune stimulation with a monomeric DAP-type PGN, tracheal cytotoxin (TCT)[5]. AMPs are quite effective against the growth of bacteria or fungi in the hemolymph[6] and perhaps in phagosomal compartments as well, but cytosolic pathogens escape these humoral defenses. Mammalian cells also express intracellular receptors that detect intracellular pathogens or their products[7]. For example, NOD1 and NOD2 sense substructures from bacterial PGN in the cell cytoplasm and activate innate immune signaling pathways[8, 9]. CARD9 is an adaptor protein that associates with NOD2 and elicits innate immune responses critical for protecting mice from *Listeria monocytogenes* infection[10]. The immune responses activated by these receptors to defend against intracellular bacterial growth are not clear, however, in either mammals or insects.

Autophagy is a highly conserved cellular mechanism in which cytoplasmic components are sequestered into double-membrane structures called autophagosomes and eventually degraded in lysosomes[11]. Autophagy is involved in diverse functions, including the removal of damaged organelles, protein turnover, the supply of nutrients under nutrient-deprived conditions, and in cell survival and death[12]. In mammalian cells, autophagy also plays a role in innate immune defenses against invading pathogens, such as group A *Streptococcus*, *Shigella flexneri*, *Mycobacterium tuberculosis*, and *Toxoplasma gondii*[13–17]. Group A *Streptococcus* is an extracellular bacteria that can also invade the host cell cytoplasm where it is rapidly sequestered into autophagosomes associated with microtubule-associated protein 1 light chain 3 (LC3, also called Atg8), resulting in its degradation in the vacuole after fusion with lysosomes[13]. *M. tuberculosis* resides in phagosomes where it interferes with phagosomal maturation and reduces the acidification of the bacteria-containing vacuole. The activation of *M. tuberculosis*-infected macrophages by interferon-γ induces autophagy; this autophagy is induced in an IRGM (immunity-related GTPase family, M; p47 GTPase)-dependent manner, and inhibits bacterial survival[14, 18]. Although these reports suggest that some intracellular pathogens induce autophagy and are controlled by autophagy in cultured cells, these studies show only limited effects on pathogen survival. Moreover, the mechanism(s) and sensor(s) mediating the induction of these autophagic antibacterial responses remain to be elucidated.

Recent studies also suggest that Toll-like receptor (TLR) signaling can promote autophagy. TLR4 stimulation promotes the colocalization of mycobacterial phagosomes with autophagosomes[19], but this is unlikely to be relevant in an infection because *M. tuberculosis* does not express any TLR4 ligands. A number of other TLR ligands also induce autophagy in cultured macrophage cell lines or murine primary macrophages[20]. It is not yet clear, however, if and how *M. tuberculosis* infections induce autophagy. Moreover, it is not yet known if autophagy plays an important role in protecting the whole animal from lethal infection by *M. tuberculosis*, Group A *Streptococcus*, or other intracellular infections.

A link between the autophagy pathway and TLR signaling is further supported by a recent report that phagocytosis of TLR agonist-coated beads promotes phagosome maturation by recruiting elements of the autophagy pathway to the phagosome [21]. Localized TLR signaling within the phagosome is therefore likely to be important for the recruitment of autophagic components.

The cytoplasmic sensor(s) that recognize bacteria invading the cytoplasm and trigger autophagy remain to be identified. Here, we demonstrate that in drosophila, PGRP-LE recognizes cytosolic *L. monocytogenes*, and is essential for inducing autophagy, which inhibits intracellular growth of the bacteria and is necessary for host survival after *L. monocytogenes* infection. In addition, the induction of autophagy after detection of the bacteria via PGRP-LE is independent of the Toll pathway and IMD pathways, suggesting the existence of a distinct innate immune pathway responsible for the induction of autophagy by a cytoplasmic sensor.

RESULTS

PGRP-LE in resistance to *L. monocytogenes* infection

We previously demonstrated that in drosophila, PGRP-LE functions as an intracellular receptor for a monomeric DAP-type PGN, TCT[5]. This finding led us to examine whether *PGRP-LE* is essential for the recognition of intracellular pathogens. We first analyzed the resistance of the *PGRP-LE* null mutant *PGRP-LE*^{112} to infection by *L. monocytogenes*, an intracellular Gram-positive bacteria that is pathogenic to mammals and drosophila and that expresses DAP-containing PGN, which is potentially recognized by PGRP-LE[4]. As indicated by survival experiments, the *PGRP-LE*^{112} mutant was hyper-susceptible to low-dose *L. monocytogenes* infection compared with wild-type (Oregon R) or *yw* flies (flies with the same genetic background as the *PGRP-LE*^{112} mutant) (Fig. 1a). Consistent with a previous report demonstrating that IMD pathway mutants are susceptible to *L. monocytogenes* infection[22], *PGRP-LC*^{7454} mutants, in which PGRP-LC, a cell surface sensor required for the activation of the IMD pathway, is hardly expressed, were also susceptible to *L. monocytogenes* infection. The survival rate of *PGRP-LE*^{112},*PGRP-LC*^{7454} double mutants following *L. monocytogenes* infection was similar to that of the *PGRP-LE*^{112} and *PGRP-LC*^{7454} mutants, suggesting that *PGRP-LE* and *PGRP-LC* do not have redundant functions in enabling resistance to *L. monocytogenes*. *L. monocytogenes* requires listeriolysin O to lyse the host phagocytic vacuole and access the cytosol[23]. The Δ*hly* strain of *L. monocytogenes*, which harbors a deletion of the gene encoding listeriolysin O, can enter host cells by phagocytosis, but is incapable of entering the cytoplasm[24]. *PGRP-LE*^{112} mutants were not susceptible to this strain, consistent with the notion that cytosolic recognition requires PGRP-LE (Fig. 1b).

L. monocytogenes infects phagocytic cells such as macrophages in mammals and hemocytes in *Drosophila*[22, 23]. PGRP-LE is expressed in hemocytes[3]. Susceptibility to *L. monocytogenes* in *PGRP-LE*^{112} mutants was rescued by expressing PGRP-LE specifically in hemocytes using the hemocyte-specific driver *hemolectin*-GAL4 (*hml*-GAL4)[25], demonstrating that *PGRP-LE* expression in hemocytes is important for resistance against *L. monocytogenes* infection (Fig. 1c). Consistent with this finding, of the expression of RNA interference (RNAi) targeting *PGRP-LE* using the *hml*-GAL4 driver induced susceptibility to *L. monocytogenes* infection (Fig. 1c). In these conditions, *hml*-GAL4-drived RNAi efficiently reduced *PGRP-LE* expression in the hemocytes (Supplementary Fig. 1, online) but did not reduce the *PGRP-LE* expression in the fat body or gut (data not shown).

Next, we examined if *PGRP-LE* is involved in suppressing bacterial growth *in vivo*. In wild-type flies, the growth of *L. monocytogenes* was relatively suppressed in both the humoral and the cellular fractions, whereas in the *PGRP-LE*^{112} mutant flies, *L. monocytogenes* growth in the cellular fraction began immediately after infection, and bacterial growth in the humoral fraction started to increase 6 h later (Supplementary Fig. 2, online). In contrast to the *PGRP-LE*^{112} mutant, bacterial growth in the humoral fraction of the *PGRP-LC*^{7454} mutant began to increase immediately after infection, but bacterial growth in the cellular fraction of the *PGRP-LC*^{7454} mutant was indistinguishable from that in wild-type flies (Supplementary Fig. 2, online). These data suggest that PGRP-LE is essential for suppressing the growth of *L. monocytogenes* within cells *in vivo*, while PGRP-LC protects the extracellular environment from these microbes.

PGRP-LE and autophagy suppress *L. monocytogenes* growth

To directly demonstrate the requirement for *PGRP-LE* in limiting the intracellular growth of *L. monocytogenes*, *ex vivo*-cultured hemocytes from drosophila larvae were infected with *L. monocytogenes* for 1 h and then incubated for 5 h in gentamicin-containing medium to kill the extracellular bacteria. *L. monocytogenes* infection of hemocytes was visualized by 4,6-

diamido-2-phenylinodole (DAPI) staining (Fig. 2a) and the number of bacteria per cell was quantified (Fig. 2b). Wild-type but not Δ*hly L. monocytogenes* produced an actin comet in hemocytes (Supplementary Fig. 3, online), suggesting that wild-type *L. monocytogenes* invaded the cytoplasm of the *ex vivo*-cultured hemocytes, which is consistent with a previous report that *L. monocytogenes* associates with actin in hemocytes derived from infected larvae[22]. The number of wild-type *L. monocytogenes* contained in the *PGRP-LE*^{112} mutant hemocytes was significantly greater than that in wild-type hemocytes (Fig. 2a, b). The number of Δ*hly* strain *L. monocytogenes* growing in *PGRP-LE*^{112} hemocytes was similar to that in wild-type hemocytes (Fig. 2b). These results suggest that PGRP-LE recognizes *L. monocytogenes* only after it enters the hemocyte cytoplasm and that phagocytic activity required for entry of the bacteria was not affected in the *PGRP-LE*^{112} mutant. PGRP-LE expression induced by the *hml*-GAL4 driver in *PGRP-LE*^{112} hemocytes rescued the growth suppression of the wild-type bacteria (Fig. 2b). These results indicate that *PGRP-LE* acts cell-autonomously in suppressing the cytosolic growth of the bacteria. In contrast to *PGRP-LE* hemocytes, those from mutant strains of Imd, the critical IMD pathway adaptor, or Relish, the key NF-κB transcription factor of the pathway, did not exhibit impaired control of intracellular *Listeria* growth (Fig. 2a,b). The control of intracellular bacterial growth was also not affected in hemocytes from larvae of *PGRP-LC*^{7454}, *MyD88*^{kra1}, a mutant of an adaptor of the Toll pathway, or J4 homozygous mutants, which lack both *Dif* and *dorsal (dl)*, key transcription factors in the Toll pathway (Fig. 2b). These results demonstrated that neither the two classical innate immune signaling pathways, nor the cell surface receptor for DAP-type PGN, are required to control the intracellular growth of *L. monocytogenes*; in contrast, the intracellular PGN receptor PGRP-LE is crucial. These results argue that some mechanism other then AMP production is essential for defending against cytosolic *L. monocytogenes*.

Several recent studies reported that autophagy functions in innate immune responses against intracellular pathogens in mammalian cells[13–18]. As AMPs do not appear necessary to control intracellular *L. monocytogenes*, we investigated whether autophagy is required for the inhibition of *L. monocytogenes* growth in hemocytes by expressing an RNAi transgene targeting drosophila *Atg5* (CG1643), an essential factor for autophagy[26, 27], with an *hml*-GAL4 driver, which efficiently reduced *Atg5* expression in hemocytes (Supplementary Fig. 1, online). *Ex vivo*-cultured hemocytes expressing *Atg5* RNAi contained higher numbers of bacteria (Fig. 2a,b). The numbers of bacteria were similarly increased in hemocytes from the *Atg1*$^{\Delta 3D}$ mutant (Fig. 2b), in which starvation-induced autophagy is completely abolished[26]. Consistent with a recent report demonstrating that autophagy limits the intracellular growth of *L. monocytogenes* in mouse embryonic fibroblast cells[28], these results indicate the essential role of autophagy in defending against *L. monocytogenes* infection. Moreover, the induction of autophagy by rapamycin treatment[29] and by the forced expression of *Atg1*[30] using the *hml*-GAL4 driver reduced the numbers of bacteria in *PGRP-LE*^{112} cells, suggesting that *PGRP-LE* acts upstream of autophagy in the resistance against *L. monocytogenes* infection (Fig. 2b).

The function of autophagy in hemocytes during innate immune responses against *L. monocytogenes* was confirmed *in vivo* by examining survival rates of flies in which the RNAi transgene against *Atg5* was expressed in hemocytes. *Atg5* RNAi flies were susceptible to wild-type *L. monocytogenes* infection, similar to *PGRP-LE*^{112} mutants, whereas they were totally resistant to the Δ*hly* strain of *L. monocytogenes* (Fig. 3a,b). In contrast, the susceptibility of the *Atg5* RNAi line and *PGRP-LE*^{112} to *Erwinia carotovora*, an extracellular Gram-negative bacteria, was not different from that of the control flies (Fig. 3c). The *PGRP-LC*^{7454} mutant was more susceptible to *E. carotovora*. This is the first demonstration that autophagy is crucial for host survival against intracellular pathogens.

Drosophila S2 cells are macrophage-like cells and are an excellent model for studying intracellular infections, especially *L. monocytogenes* infection[31, 32]. S2 cells had no detectable

expression of PGRP-LE (Supplementary Fig. 4, online), thus we compared *L. monocytogenes* infection in S2 cells and S2 cells stably transfected with a metallothionein promoter-PGRP-LE expression plasmid[5]. Incubation for 1.5 h with wild-type *L. monocytogenes*, followed by additional incubation for 6 h in medium containing gentamicin and 100 μM $CuSO_4$ to induce PGRP-LE reduced the number of bacteria within the cells to numbers similar to that observed following infection with the Δ*hly* strain (Fig. 4a). *Atg5* knockdown by RNAi in S2 cells expressing PGRP-LE (Supplementary Fig. 4b, online) restored the numbers of bacteria to those seen in S2 cells (Fig. 4a). Infection of S2 cells expressing PGRP-LE with wild-type *L. monocytogenes* induced AMP expression in a PGRP-LE dependent manner (Supplementary Fig. 5a, online). This induction was totally dependent on *imd*, a key factor in the Imd pathway (Supplementary Fig. 5b, online). In contrast to AMP induction, PGRP-LE mediated suppression of bacterial growth was not affected by the knockdown of *Relish* or *imd* (Fig. 4a and data not shown). PGRP-LE–mediated suppression of bacterial growth was also not affected by the knockdown of *Dif* and *dl* (Fig. 4a). On the other hand, AMP induction was not affected by *Atg5* knockdown, suggesting that the autophagy pathway is not essential for AMP induction in *L. monocytogenes* infection (Supplementary Fig. 5b, online). Knockdown of *Relish*, *Dif/dl*, and *Atg5* expression had no effect on the number of Δ*hly* strain bacteria in either S2 cells or S2 cells expressing PGRP-LE (Fig. 4a), suggesting that these genes were not involved in phagocytic entry of the bacteria. These results suggest that the autophagy pathway but not NF-κB transcription factors (Relish, Dif, Dorsal) is required for PGRP-LE–mediated suppression of intracellular *L. monocytogenes* growth. Consistent with the results suggesting the importance of the autophagy pathway in the PGRP-LE–mediated suppression of intracellular *Listeria* growth, a time-course evaluation of the intracellular growth of the bacteria in S2 cells expressing PGRP-LE revealed a decrease in the number of intracellular wild-type, but not Δ*hly*, *L. monocytogenes*, 2.5 hours after infection (0.5 h infection plus 2 h with gentamicin). At later time points, the bacteria remained at low numbers in the S2-PGRP-LE cell line, but multiplied robustly in S2 cells that did not express PGRP-LE (Supplementary Fig. 6, online).

PGRP-LE functions as an intracellular receptor by detecting peptidoglycan fragments[5], and is essential for suppressing intracellular bacterial growth. To test the possibility that PGRP-LE detects bacteria that invade host cell cytoplasm, S2 cells expressing yellow fluorescent protein (YFP)-tagged PGRP-LE[5] were infected with wild-type or Δ*hly* strain *L. monocytogenes*, and assayed by confocal fluorescence microscopy (Fig. 4b,c). With no bacterial infection, YFP-tagged PGRP-LE was dispersed throughout the cytoplasm[5]. With wild-type bacterial infection, however, YFP-tagged PGRP-LE accumulated around the bacteria (Fig. 4b); in contrast, infection with the Δ*hly* strain, which cannot enter the cytoplasm, did not result in the accumulation of YFP-tagged PGRP-LE around bacteria (Fig. 4c). These results suggest that PGRP-LE directly detects invading *L. monocytogenes* after it enters the cytoplasm.

Autophagy induction via the cytoplasmic sensor PGRP-LE

These data suggest that intracellular PGRP-LE is responsible for detecting invading *L. monocytogenes* and for inducing autophagy. To test this possibility, we examined whether *L. monocytogenes* invading the cell cytoplasm is surrounded by autophagosomes in a PGRP-LE–dependent manner. A fusion protein of LC3 with green fluorescent protein (GFP)[33] was expressed under the control of an actin promoter in S2 cells or S2 cells expressing PGRP-LE, and the distribution of GFP-LC3 was examined using confocal fluorescence microscopy. GFP-LC3 is an autophagosome-specific membrane marker that is detected in ring- or dot- shaped structures when autophagosomes are formed in mammalian cell cytoplasm[13, 14, 33] and in drosophila fat body cells[27]. In contrast to a previous report that TLR4-dependent induction of autophagy by lipopolysaccharide treatment in a murine macrophage cell line is maximal 12 to 16 h after LPS stimulation[19], dot-shaped or ring-shaped GFP-LC3 signals were observed in

S2 cells expressing PGRP-LE after only 1.5 h incubation (0.5 h of the initial incubation plus an additional 1 h in the presence of gentamicin) with wild-type *L. monocytogenes* (Fig. 5a,c). The number of GFP-LC3 dots observed in Δ*hly* strain-infected cells was near the background quantity (Fig. 5a). In S2 cells, in which no detectable PGRP-LE is expressed, wild-type *L. monocytogenes* infection did not increase GFP-LC3 dot formation (Fig. 5a). These results suggest that PGRP-LE is essential for the GFP-LC3 dot formation caused by the invasion of wild-type *L. monocytogenes* into the cell cytoplasm. Treatment of Rapamycin, an inhibitor of autophagy inhibitory factor TOR[29], of S2 cells induced a similar frequency of GFP-LC3 dots as in S2 cells expressing PGRP-LE (Fig. 5a), suggesting that dot or ring-shaped GFP-LC3 formation *per se* was not affected by the lack of PGRP-LE expression. In S2 cells expressing PGRP-LE and infected with wild-type *L. monocytogenes*, one or several bacteria were often surrounded by ring-shaped GFP-LC3 dots (Fig. 5b,c). Colocalization of the wild-type bacteria with GFP-LC3 dots in S2 cells expressing PGRP-LE was detected after 0.5 h incubation with bacteria, and the frequency of the colocalization after 1.5 h incubation (0.5 h incubation with bacteria plus 1 h in the presence of gentamicin) was 57.7±5.3%, which was significantly higher than that in wild-type bacteria-infected S2 cells (7.9± 6.9%) (Fig. 5b).

During the autophagic processes, cytosolic LC3 (LC3-I) is conjugated on its C-terminus with phosphatidylethanolamine, and the lipidated LC3 (LC3-II) localizes to the autophagic membrane[34]. Therefore, the amount of LC3-II correlates with the number of autophagosomes. After infection, the amount of GFP-LC3-II increased markedly in S2 cells expressing PGRP-LE, whereas there was no change in the amount of GFPLC3-II in infected parental S2 cells that did not express PGRP-LE (Fig. 5d). Rapamycin treatment induced an increase in the amount of GFP-LC3-II in both cell types (Fig. 5d). These observations suggest that PGRP-LE is not essential for autophagosome formation *per se*, but that autophagosome formation is induced via PGRP-LE when *L. monocytogenes* invades the cytoplasm. As expected, *Atg5* knockdown prevented the conversion of LC3-I to LC3-II upon bacterial infection or rapamycin treatment (Fig. 5d).

Next, we investigated whether the GFP-LC3-expressing structures that surround *L. monocytogenes* have the typical characteristics of autophagosomes. One hour after infection (0.5 h of the initial incubation plus an additional 0.5 h in the presence of gentamicin), we examined GFP-LC3 dots in S2 cells expressing PGRP-LE and GFP-LC3 by fluorescence microscopy (Fig. 5e); the same fields were also observed under electron microscopy (Fig. 5f–i). We noted double-membrane structures engulfing the bacteria (Fig. 5g–i), suggesting that PGRP-LE recognition of *L. monocytogenes* in the cytoplasm induces conventional autophagy around the bacteria.

We then determined whether endogenously expressed PGRP-LE is essential for inducing autophagy following *L. monocytogenes* infection of hemocytes. GFP-LC3 was expressed using a *heat shock*-GAL4 driver in the third instar larvae, and hemocytes from the larvae were cultured *ex vivo* with *L. monocytogenes*. After 1 h incubation with wild-type *L. monocytogenes*, followed by an additional 1 h incubation in gentamicin-containing medium, GFP-LC3 dots were observed in *L. monocytogenes*-infected wild-type hemocytes, and confocal microscopic analysis revealed that infected *L. monocytogenes* were surrounded by GFP-LC3-expressing structures (Fig. 5j, k). In contrast, GFP-LC3 dot formation frequency was similar in uninfected and infected *PGRP-LE*^{112} hemocytes (Fig. 5k). This result was not due to decreased phagocytic activity in *PGRP-LE*^{112} hemocytes, because similar numbers of Δ*hly* strain *L. monocytogenes* infected *PGRP-LE*^{112} and wild-type hemocytes (Fig. 2b). Similarly, this result was not due to a generalized defect in autophagosome formation in *PGRP-LE*^{112} hemocytes as the frequency and morphology of the GFP-LC3 dots induced by rapamycin treatment was similar in *PGRP-LE*^{112} and wild-type hemocytes (Fig. 5k and Supplementary Fig. 7, online). GAL4-dependent RNAi transgene targeting of *Atg5* greatly decreased the

number of GFP-LC3 dots per infected cells to that in uninfected cells (Fig. 5k). GFP-LC3 dots were rarely detected in Δ*hly* strain-infected hemocytes (Fig. 5k). Together, these data indicate that *L. monocytogenes* invasion of the cytoplasm induces autophagy in a manner dependent on endogenously expressed functional PGRP-LE.

PGRP-LE-dependent induction of autophagy in hemocytes was confirmed by immunoblotting studies that revealed the modification of GFP-LC3. Wild-type and *PGRP-LE*^{112} hemocytes expressing GFP-LC3, or hemocytes that express a RNAi transgene targeting *Atg5* were incubated *ex vivo* with wild-type *L. monocytogenes* for 0.5 h, followed by an additional incubation for 2 h in gentamicin-containing medium; thereafter modification of GFP-LC3 was analyzed by immunoblotting using an anti-GFP antibody. *L. monocytogenes* infection or rapamycin treatment of wild-type hemocytes enhanced the intensity of the processed form of GFP-LC3, whereas infection had no effect on GFP-LC3 processing in the *PGRP-LE*^{112} mutant or *Atg5* RNAi hemocytes (Fig. 5l). These results indicate that *PGRP-LE* is required for the induction of autophagy in response to *L. monocytogenes* infection.

PGRP-LE–mediated AMP induction in response to *L. monocytogenes* infection in S2 cells is dependent on the IMD pathway (Supplementary Fig. 5, online). PGRP-LE–mediated suppression of intracellular bacterial growth in S2 cells and hemocytes, however, was not dependent on the IMD and Toll pathways. We therefore examined whether PGRP-LE–mediated autophagosome formation was dependent on the IMD and/or Toll signaling pathways. The number of GFP-LC3 dots per cell was quantified in wild-type *Listeria*-infected S2 cells that expressed both PGRP-LE and GFP-LC3. Knockdown of *imd, Relish, MyD88, or both Dif and dorsal* by RNAi in wild-type *Listeria*-infected S2 cells expressing PGRP-LE and GFP-LC3 did not affect the formation of GFP-LC3 dots, but *Atg5* knockdown decreased the number of LC3 dots per cell (Fig. 5m). Knockdown of PGRP-LC, the membrane-associated PGRP that senses bacteria on the surface of the cell membrane, also did not affect GFP-LC3 dot formation (Fig. 5m). These results suggest that the PGRP-LE–mediated autophagosome formation is independent of IMD and Toll pathways, consistent with other data indicating that PGRP-LE–mediated suppression of intracellular bacterial growth does not involve with these pathways (Fig. 4a).

Autophagy induced by DAP-type PGN

PGRP-LE recognizes TCT and DAP-containing PGN[4, 5]. We next examined whether TCT and PGN induce autophagy in the cell cytoplasm. Highly purified TCT[35], highly purified DAP-type PGN, or highly purified lysine-type PGN was transfected into S2 cells expressing PGRP-LE and GFP-LC3 using a calcium phosphate transfection method, and GFP-LC3 dots were quantified after 2 h of incubation. TCT, DAP-, or lysine-type PGN increased the number of GFP-LC3 dots per cell to a frequency similar to that in *L. monocytogenes*-infected cells (Fig. 6a). In contrast, lysine-type PGN but not TCT or DAP-type PGN induced an increase in the number of GFP-LC3 dots in S2 cells lacking PGRP-LE (Fig. 6a). Similar results were observed using chemically synthesized TCT (data not shown). Transfection of synthetic desmuramylpeptide, a peptidoglycan fragment containing DAP, FK156 (D-lactyl-L-Ala-γ-D-Glu-meso-DAP-Gly)[36], or its derivative, FK565 (haptanoyl-γ-D-Glu-meso-DAP-D-Ala), did not increase the number of GFP-LC3 dots in S2 cells expressing PGRP-LE (data not shown). Correlative FM-EM analysis revealed that the TCT-induced GFP-LC3–expressing structures have double-membrane structures typical of autophagosomes (Supplementary Fig. 8a,b, online). These results suggest that autophagy induction mediated by TCT and DAP-type PGN, but not lysine-type PGN, is dependent on PGRP-LE. We also examined GFP-LC3 dot formation in response to TCT, DAP-type, or lysine-type PGN in *ex vivo*-cultured hemocytes, although the precise mechanism of cytoplasmic delivery of PGN in hemocytes is not clear. The TCT- and DAP-type PGN-dependent formation of GFP-LC3 dots was suppressed in

PGRP-LE^{112} mutant hemocytes compared to wild-type counterparts, but lysine-type PGN-dependent formation of GFP-LC3 dots was not affected in *PGRP-LE*^{112} mutant hemocytes (Fig. 6b, Supplementary Fig. 8c–h). These results suggest that PGRP-LE is crucial for the induction of autophagosome formation in response to TCT and DAP type-PGN, but not to lysine-type PGN. Together, these findings indicate that PGRP-LE likely recognizes DAP-type PGN of *L. monocytogenes* to induce autophagy.

DISCUSSION

Recent evidence indicates the importance of autophagy as a defense against intracellular pathogens, and the mechanism(s) underlying the induction of autophagy during pathogen infection is a central issue. The results of the present study demonstrate that PGRP-LE, through its ability to induce autophagy and prevent the intracellular bacterial growth, is essential in drosophila for resistance against *L. monocytogenes*. These findings indicate that the induction of autophagy, as an innate defense mechanism targeting intracellular pathogens, is activated by intracellular microbial sensors. In mammalian cells, the NOD-like receptors (or other intracellular microbial receptors) may sense bacterial invasion of the cytoplasm and induce autophagy in response to cytoplasm-invading bacterial infection. In fact, autophagy induction during *L. monocytogenes* infection of mouse embryonic fibroblast cells requires the expression of listeriolysin O[28], suggesting that the sensing of *L. monocytogenes* in mammalian cells also occurs in the cytoplasm.

In primary hemocytes and S2 cells, both DAP-type and lysine-type PGN induced autophagy, although PGRP-LE was responsible only for the autophagy induction stimulated by the DAP-type PGN. These results strongly suggest that other cytoplasmic sensor(s) detect invading bacteria with cell walls containing lysine-type PGN. In mammals, autophagy has also been linked to the resistance against parasites, such as *Toxoplasma gondii*, and viruses[12]. Although the fundamental mechanisms linking these pathogens with the autophagy machinery might be similar to that used in bacterial infections, it is likely that the host cells utilize distinct sensors to induce autophagy in response to each type of pathogen.

Although the molecular mechanisms and signaling pathways leading to starvation-induced autophagy are well-studied, the signaling pathways that induce autophagy upon pathogen infection is just beginning to be clarified. In contrast to AMP induction, PGRP-LE-mediated induction of autophagy was independent of the Toll and IMD pathways. However, autophagy inducted by LPS through TRIF-dependent TLR4 signaling overcomes an *M. tuberculosis*-mediated phagosome block and promotes its colocalization with autophagosomes[19]. PGRP-LE has an RHIM-like motif, which is similar to the receptor-interacting protein homotypic interaction motif present in TRIF and receptor-interacting protein 1 (RIP1)[5]. This motif is required for the interaction between these two proteins, and for TRIF- and TLR3-induced NF-κB activation[37, 38]. It is possible that an unidentified factor with an RHIM-like motif interacts with PGRP-LE to activate the signaling pathway to induce autophagy.

Autophagy has been shown to be essential for the defense against several kinds of pathogens in cultured cells[13–17]. Thus, this report opens the door to investigating the connection between intracellular pattern recognition receptors and autophagy as an immune response, and the signaling pathways involved in both insects and mammals.

Methods

Fly strains

Stocks were raised on a standard cornmeal-yeast agar medium at 25°C. The following strains used in this study are described elsewhere: *ywPGRP-LE*^{112} (*PGRP-LE*^{112})[3], *w;;PGRP-*

LC^{7454} (*PGRP-LC*^{7454})[39], *Relish*^{E20} (*Relish*^{E20})[3], *w;;Atg1*$^{\Delta 3D}$ (*Atg1*$^{\Delta 3D}$)[26], *w;;hml*-GAL4 (*hml*-GAL4)[25], *w;cg*-GAL4 (*cg*-GAL4)[30], *w*;UAS-PGRP-LE (UAS-PGRP-LE) [4], *yw*UAS-Atg5 IR (UAS-Atg5 IR)[26], *yw*;;UAS-Atg1^{6B} (UAS-Atg1)[30], and *w*;UAS-GFP-LC3 (UAS-GFP-LC3)[27].

Survival experiments

Bacterial infections were performed by injecting approximately 70 nl per fly of a dilution of cultured bacterial strains (1/100,000 dilution of an *L. monocytogenes* suspension or *E. carotovora* suspension; A_{600} = 1.0), which resulted in the injection of approximately 10 bacteria per fly. All survival experiments were performed with 30 flies for each genotype tested at 28°C for the *L. monocytogenes* injections, or 25°C for the *E. carotovora* injections. Surviving flies were transferred daily into fresh vials.

L. monocytogenes infection of *ex vivo*-cultured hemocytes

Third instar larvae were dissected in 10% fetal bovine serum-containing Schneider's *Drosophila* medium mounted on concanavalin A-treated glass slides. After a few minutes incubation to allow the hemocytes to attach to the glass slide, the medium was exchanged with new media, and a suspension of *L. monocytogenes* grown to mid-log phase was added to the culture (approximately 20 bacteria per cell), followed by 1 h incubation at 28°C. Cells were washed and further incubated at 28°C for the indicated time in Schneider's *Drosophila* medium containing 10% fetal bovine serum and 10 μg/ml gentamicin. Cells were then fixed with 2% paraformaldehyde for immunohistochemical analyses. For the induction of GFP-LC3, third instar larvae were heat-shocked (at 37°C for 20 min) 12 h before hemocyte isolation.

Bacterial strains

The following *L. monocytogenes* strains were used in this study: wild-type strain, 10403S; Δ*hly* strain, DP-L2161[31]; GFP-expressing wild-type strain, DH-L1039; and GFP-expressing Δ*hly* strain, DH-L1137[32]. *E. carotovora carotovora* 15 was used in the survival experiments.

Peptidoglycans

The DAP-type and the Lys-type peptidoglycans were highly purified from *Lactobacillus plantarum* ATCC 8014 and *Staphylococcus epidermidis* ATCC 155, respectively, according to the previously reported method[40]. Purity was confirmed by amino acid analysis. Highly purified TCT was described previously[35]. Chemically synthesized TCT was prepared using an orthogonally protected *meso*-diaminopimelic acid (*meso*-DAP) containing tetrapeptide (L-Ala-γ-D-Glu(OBn)-*meso*-DAP(*N*-Z, OBn)-D-Ala(OBn)) and a disaccharide (4,6-*O*-benzylidene-3-*O*-benzyl-GlcNAc-(β1-4)-MurNAc(anh)). After condensation of the disaccharide and the tetrapeptide with 1-ethyl-3-(3-dimethylaminopropyl)carbodiimide hydrochloride (water-soluble carbodiimide hydrochloride; WSCD•HCl), 1-hydroxybenzotriazole (HOBt), triethylamine, in *N*,*N*-dimethyl formamide (DMF), deprotection of all the protecting groups by hydrogenation (H_2 (20 kg/cm^2), $Pd(OH)_2$, in tetrahydrofuran) gave TCT. The molecular weight of TCT was confirmed with ESI-TOF-MS (negative) *m/z* 920.4 $[M-H]^-$; HRMS-ESI TOF-MS (positive) *m/z* calcd. for $C_{29}H_{48}N_6O_{16}$, $[M+H]^+$ 922.3893, found 922.3898. The synthetic desmuramylpeptide, a peptidoglycan fragment containing DAP, FK156 [36] (D-lactyl-L-Ala-γ-D-Glu-meso-DAP-Gly) and its derivative, FK565 (haptanoyl-γ-D-Glu-meso-DAP-D-Ala) was supplied by Astellas Pharmaceutical (formerly Fujisawa and Yamanouchi).

RNA interference in S2 cells

The double-stranded RNA used in the RNAi experiments was synthesized as previously described[5]. Templates for double-stranded *Atg5* RNA were amplified with the primers 5'-

TAATACGACTCACTATAGGGCAAATAAGGAACATGGCC-3' and 5'-TAATACGACTCACTATAGGGTCAGGCAGGACATGTAG-3'. Double-stranded RNA was transfected into S2 cells as previously described[5].

L. monocytogenes infection of S2 cells and measurement of the number of intracellular bacteria

Cultures (1×10^6 cells/ml) were incubated for 18 h, and 50 nM water-soluble cholesterol was added to the culture as previously described[30]. After 30 min incubation, a suspension of *L. monocytogenes* (approximately 20 bacteria/cell unless otherwise described) was added and the cells were incubated at 28°C for 1.5 h in the case of infection with 20 bacteria/cell. Cells were then washed with phosphate buffered saline (PBS), and incubated in Schneider's drosophila medium containing 100 μM $CuSO_4$ and 10 μg/ml gentamicin for 6 h. After washing with PBS, cells were dispersed in water to release bacteria from the cytoplasm of the S2 cells. Samples were then plated on Brain-Heart-Infusion plates to measure colony-forming units.

Immunohistochemistry

Fixed hemocytes or S2 cells were washed with PBS and stained with anti-GFP (Medical & Biological Laboratories) in PBS containing 1% bovine serum albumin and 0.1% Triton X-100 for 1 h, and then with fluorescein isothiocyanate-labeled anti-rabbit IgG (Molecular Probes), rhodamine-labeled phalloidin (Molecular Probes) for 1 h when required, followed by 10 min DAPI staining (Sigma).

Immunoblotting—S2 cells were infected with wild-type *L. monocytogenes* (approximately 500 bacteria/cell) for 0.5 h at 28°C, and further incubated in gentamicin-containing medium for 1 h at 28°C. *Ex vivo*-cultured hemocytes were infected with wild-type *L. monocytogenes* (approximately 200 bacteria/cell) for 1 h at 28°C, washed with PBS, and further incubated in gentamicin-containing medium for 2 h at 28°C. For immunoblotting, cells were washed with PBS, and lysed with buffer containing 50 mM Tris-HCl, 2% sodium dodecyl sulfate, 10% glycerol, and 100 mM β-mercaptoethanol. Lysate from the same number of cells was loaded on 10% sodium dodecyl sulfate-polyacrylamide gels and transferred to polyvinylidene membranes, and subjected to immunoblot analysis using antibodies against either GFP (Medical & Biological Laboratories), α-tubulin (Santa Cruz Biotechnology), β-tubulin (Hybridoma Bank), or V5-tag (Invitrogen). Blots were visualized using ECL-Western Blotting Analysis System (GE Healthcare).

Correlative FM-EM

Correlative fluorescence microscopy-electron microscopy (FM-EM) allows individual cells to be examined both in an overview with FM and in a detailed subcellular structure view with EM. For observation by FM-EM, S2 cells cultured on glass-bottom dishes (MatTek) were fixed with 2% paraformaldehyde and 2.5% glutaraldehyde in 0.1 M sodium cacodylate (pH 7.4) for 2 h, and then examined using a confocal laser scanning microscope. The same specimens were further incubated with 2.5% glutaraldehyde and 2% formaldehyde in 0.1 M sodium cacodylate (pH 7.4) at 4°C overnight. After three washings with 0.1 M sodium cacodylate (pH 7.4) containing 7% sucrose, the samples were postfixed with 1% osmium tetroxide and 0.5% potassium ferrocyanide in the same buffer for 1 h, washed with distilled water three times, dehydrated in ethanol, and embedded in Epon812 (TAAB Laboratories Equipment, Ltd.). Ultrathin sections of the cell (70 nm thick) were stained with saturated uranyl acetate and Reynolds lead citrate solution. Electron micrographs were taken with a JEOL JEM-1011 transmission electron microscope (JEOL, Ltd.).

Supplementary Material

Refer to Web version on PubMed Central for supplementary material.

Acknowledgements

We thank D. A. Portnoy (University of California, Berkeley) and D. E. Higgins (Harvard Medical School) for *L. monocytogenes* strains; L. W. Cheng (University of California, Berkeley) for the S2 cell *L. monocytogenes* infection protocol; T. P. Neufeld (University of Minnesota) for $Atg1^{\Delta 3D}$, UAS-*Atg5* IR, UAS-Atg1, and UAS-GFP-LC3; D. Hultmark (Umeå University) for $Relish^{E20}$; K. Anderson (Cornell University) for $PGRP\text{-}LC^{7454}$; A. Goto for *hml*-GAL4; the Bloomington Stock Center, Drosophila Genetic Resource Center at the Kyoto Institute of Technology and the Genetic Strain Research Center of National Institute of Genetics for fly stocks; and S. Iwanaga (a professor emeritus, Kyushu University), M. Mitsuyama (Kyoto University), A. Yamamoto (Nagahama Institute of Bio-Science and Technology), and S. Natori (a professor emeritus, The University of Tokyo) for helpful discussions. This work was supported by Grants-in-Aid for Scientific Research from the Ministry of Education, Culture, Sports, Science, and Technology of Japan; the Japan Society for the Promotion of Science; the Program for the Promotion of Basic Research Activities for Innovative Biosciences (PROBRAIN); the NIH grant (AI074958); and the Naito Foundation and from the NIH (AI60025 and AI074958) to N.S.

References

1. Lemaitre B, Hoffmann J. The host defense of *Drosophila melanogaster*. Annu. Rev. Immunol 2007;25:697–743. [PubMed: 17201680]
2. Ferrandon D, Imler J-L, Hetru C, Hoffmann JA. The *Drosophila* systemic immune response: sensing and signaling during bacterial and fungal infections. Nat. Rev. Immunol 2007;7:862–874. [PubMed: 17948019]
3. Takehana A, et al. Peptidoglycan recognition protein (PGRP)-LE and PGRP-LC act synergistically in *Drosophila* immunity. EMBO J 2004;23:4690–4700. [PubMed: 15538387]
4. Takehana A, et al. Overexpression of a pattern-recognition receptor, peptidoglycan-recognition protein-LE, activates imd/relish-mediated antibacterial defense and the prophenoloxidase cascade in *Drosophila* larvae. Proc. Natl. Acad. Sci. USA 2002;99:13705–13710. [PubMed: 12359879]
5. Kaneko T, et al. PGRP-LC and PGRP-LE have essential yet distinct functions in the drosophila immune response to monomeric DAP-type peptidoglycan. Nat. Immunol 2006;7:715–723. [PubMed: 16767093]
6. Lemaitre B, Reichhart J-M, Hoffmann JA. *Drosophila* host defense: Differential induction of antimicrobial peptide genes after infection by various classes of microorganisms. Proc. Natl. Acad. Sci. USA 1997;94:14614–14619. [PubMed: 9405661]
7. Kanneganti T-D, Lamkanfi M, Núñez G. Intracellular NOD-like receptor in host defense and disease. Immunity 2007;27:549–559. [PubMed: 17967410]
8. Chaput C, Boneca IG. Peptidoglycan detection by mammals and flies. Microbes Infect 2007;9:637–647. [PubMed: 17383922]
9. Delbridge LM, O'Riordan MXD. Innate recognition of intracellular bacteria. Curr. Opin. Immunol 2007;19:10–16. [PubMed: 17126540]
10. Hsu YM, et al. The adaptor protein CARD9 is required for innate immune responses to intracellular pathogens. Nat. Immunol 2007;8:198–205. [PubMed: 17187069]
11. Mizushima N. Autophagy: process and function. Genes Dev 2007;21:2861–2873. [PubMed: 18006683]
12. Levine B, Deretic V. Unveiling the roles of autophagy in innate and adaptive immunity. Nat. Rev. Immunol 2007;7:767–777. [PubMed: 17767194]
13. Nakagawa I, et al. Autophagy defends cells against invading Group A *Streptococcus*. Science 2004;306:1037–1040. [PubMed: 15528445]
14. Gutierrez MG, et al. Autophagy is a defense mechanism inhibiting BCG and *Mycobacterium tuberculosis* survival in infected macrophages. Cell 2004;119:753–766. [PubMed: 15607973]
15. Ogawa M, et al. Escape of intracellular *Shigella* from autophagy. Science 2005;307:727–731. [PubMed: 15576571]

16. Ling YM, et al. Vacuolar and plasma membrane stripping and autophagic elimination of *Toxoplasma gondii* in primed effector macrophages. J. Exp. Med 2006;203:2063–2071. [PubMed: 16940170]
17. Andrade RM, Weaaendarp M, Gubbels M-J, Striepen B, Subauste CS. CD40 induces macrophage anti-*Toxoplasma gondii* activity by triggering autophagy-dependent fusion of pathogen-containing vacuoles and lysosomes. J. Clin. Invest 2006;116:2366–2377. [PubMed: 16955139]
18. Singh SB, Davis AS, Taylor GA, Deretic V. Human IRGM induces autophagy to eliminate intracellular mycobacteria. Science 2006;313:1438–1441. [PubMed: 16888103]
19. Xu Y, et al. Toll-like receptor 4 is a sensor for autophagy associated with innate immunity. Immunity 2007;27:135–144. [PubMed: 17658277]
20. Delgado MA, Elmaoued RA, Davis AS, Kyei G, Deretic V. Toll-like receptors control autophagy. EMBO J. 2008 March 13;advance online publication
21. Sanjuan MA, et al. Toll-like receptor signalling in macrophages links the autophagy pathway to phagocytosis. Nature 2007;450:1253–1257. [PubMed: 18097414]
22. Mansfield BE, Dionne MS, Schneider DS, Freitag NE. Exploration of host-pathogen interactions using *Listeria monocytogenes* and *Drosophila melanogaster*. Cell Microbiol 2003;5:901–911. [PubMed: 14641175]
23. Hamon M, Bierne H, Cossart P. *Listeria monocytogenes*: a multifaceted model. Nat. Rev. Microbiol 2006;4:423–434. [PubMed: 16710323]
24. Jones S, Portnoy DA. Characterization of *Listeria monocytogenes* pathogenesis in a strain expressing Perfringolysin O in place of Listeriolysin O. Infect. Immun 1994;62:5608–5613. [PubMed: 7960143]
25. Goto A, Kadowaki T, Kitagawa Y. Drosophila hemolectin gene is expressed in embryonic and larval hemocytes and its knock down causes bleeding defects. Dev. Biol 2003;264:582–591. [PubMed: 14651939]
26. Scott RC, Schuldiner O, Neufeld TP. Role and regulation of starvation-induced autophagy in the *Drosophila* fat body. Dev. Cell 2004;7:167–178. [PubMed: 15296714]
27. Rusten TE, et al. Programmed autophagy in the *Drosophila* fat body is induced by ecdysome through regulation of the PI3K pathway. Dev. Cell 2004;7:179–192. [PubMed: 15296715]
28. Py BF, Lipinski MM, Yuan J. Autophagy limits *Listeria monocytogenes* intracellular growth in the early phase of primary infection. Autophagy 2007;3:117–125. [PubMed: 17204850]
29. Noda T, Ohsumi Y. Tor, a phosphatidylinositol kinase homologue, controls autophagy in yeast. J. Biol. Chem 1998;273:3963–396. [PubMed: 9461583]
30. Scott RC, Juhasz G, Neufeld TP. Direct induction of autophagy by Atg1 inhibits cell growth and induces apoptotic cell death. Curr. Biol 2007;17:1–11. [PubMed: 17208179]
31. Cheng LW, Portnoy DA. *Drosophila* S2 cells: an alternative infection model for *Listeria monocytogenes*. Cell. Microbiol 2003;5:875–885. [PubMed: 14641173]
32. Agaisse H, et al. Genome-wide RNAi screen for host factors required for intracellular bacterial infection. Science 2005;309:1248–1251. [PubMed: 16020693]
33. Mizushima N, Yamamoto A, Matsui M, Yoshimori T, Ohsumi Y. In vivo analysis of autophagy in response to nutrient starvation using transgenic mice expressing a fluorescent autophagosome marker. Mol. Biol. Cell 2004;15:1101–1111. [PubMed: 14699058]
34. Kabeya Y, et al. LC3, a mammalian homologue of yeast Apg8p, is localized in autophagosome membranes after processing. EMBO J 2000;19:5720–5728. [PubMed: 11060023]
35. Kaneko T, et al. Monomeric and polymeric gram-negative peptidoglycan but not purified LPS stimulate the *Drosophila* IMD pathway. Immunity 2004;20:637–649. [PubMed: 15142531]
36. Kitaura Y, et al. N_2-(-D-glutamyl)-*meso*-2L,2'D-diaminopimelic acid as the minimal prerequisite structure of FK-156: its acyl derivatives with potent immunostimulating activity. J. Med. Chem 1982;25:335–337. [PubMed: 7069711]
37. Sun X, Yin J, Starovansnik MA, Fairbrother WJ, Dixit VM. Identification of a novel homotypic interaction motif required for the phosphorylation of receptor-interacting protein (RIP) by RIP3. J. Biol. Chem 2002;277:9505–9511. [PubMed: 11734559]
38. Meylan E, et al. RIP1 is an essential mediator of Toll-like receptor 3-induced NF-κB activation. Nat. Immunol 2004;5:503–507. [PubMed: 15064760]

39. Gottar M, et al. The *Drosophila* immune response against Gram-negative bacteria is mediated by a peptidoglycan recognition protein. Nature 2002;416:640–644. [PubMed: 11912488]

40. Kotani S, Watanabe Y, Shimono T, Kinoshita F, Narita T. Immunoadjuvant activities of peptidoglycan subunits from the cell walls of *Staphylococcus aureus* and *Lactobacillus plantarum*. Biken J 1975;18:93–103. [PubMed: 1180873]

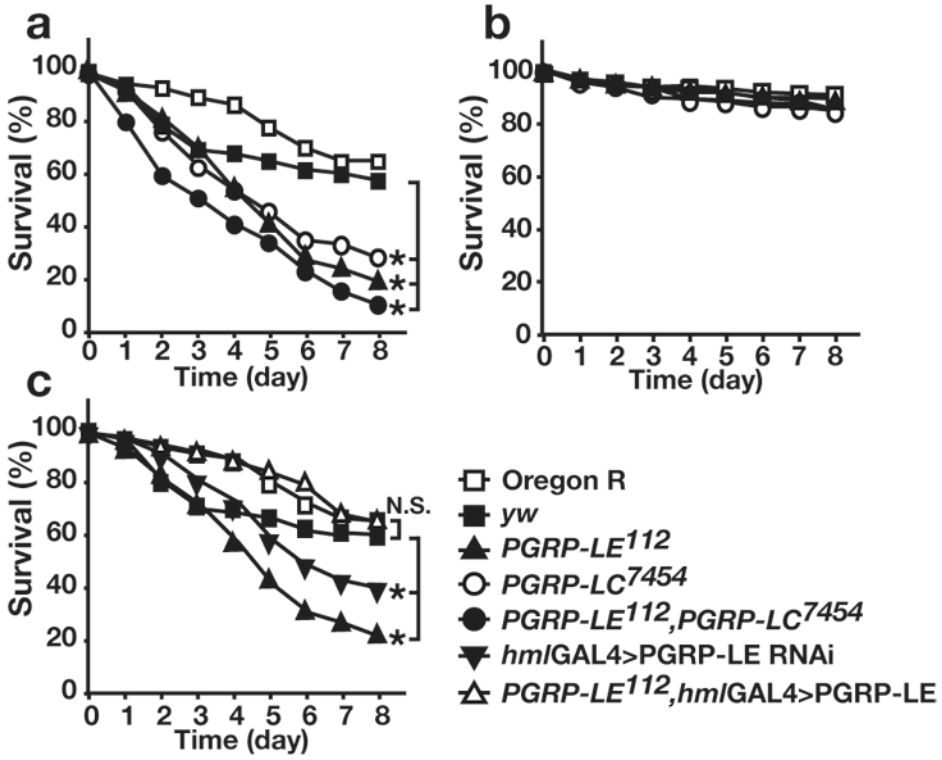

Figure 1.

PGRP-LE in hemocytes is essential for resistance against L. monocytogenes infection in vivo. (**a,b**) Survival rate of wild-type (Oregon R) flies, *yw* flies, *ywPGRP-LE*^{112} (*PGRP-LE*^{112}), *w;;PGRP-LC*^{7454} (*PGRP-LC*^{7454}), and *ywPGRP-LE*^{112},*PGRP-LC*^{7454} double-mutant flies (*PGRP-LE*^{112},*PGRP-LC*^{7454}), after (**a**) wild-type or (**b**) Δ*hly L. monocytogenes* injections. (**c**) Survival rate of Oregon R, *yw*, *ywPGRP-LE*^{112} (*PGRP-LE*^{112}), UAS-PGRP-LE IR/+; *hml*-GAL4/+, (*hml*-GAL4>PGRP-LE RNAi) and *ywPGRP-LE*^{112}; UAS-PGRP-LE/+;*hml*-GAL4/+ (*PGRP-LE*^{112}, *hml*-GAL4>PGRP-LE) flies after wild-type *L. monocytogenes* injections. All experiments were performed at 28°C. The average survival rate of four independent experiments is shown. In each experiment, >30 flies of the indicated genotypes were examined at the same time. * $P<0.01$ (Wilcoxon-Mann-Whitney test) (P=0.0006, 0.0043, 0.0043, *yw* versus *PGRP-LE*^{112}, *PGRP-LC*^{7454}, *PGRP-LE*^{112},*PGRP-LC*^{7454} flies, respectively in (a) P=0.0095 *yw* versus *hml*-GAL4>PGRP-LE RNAi flies in (c))

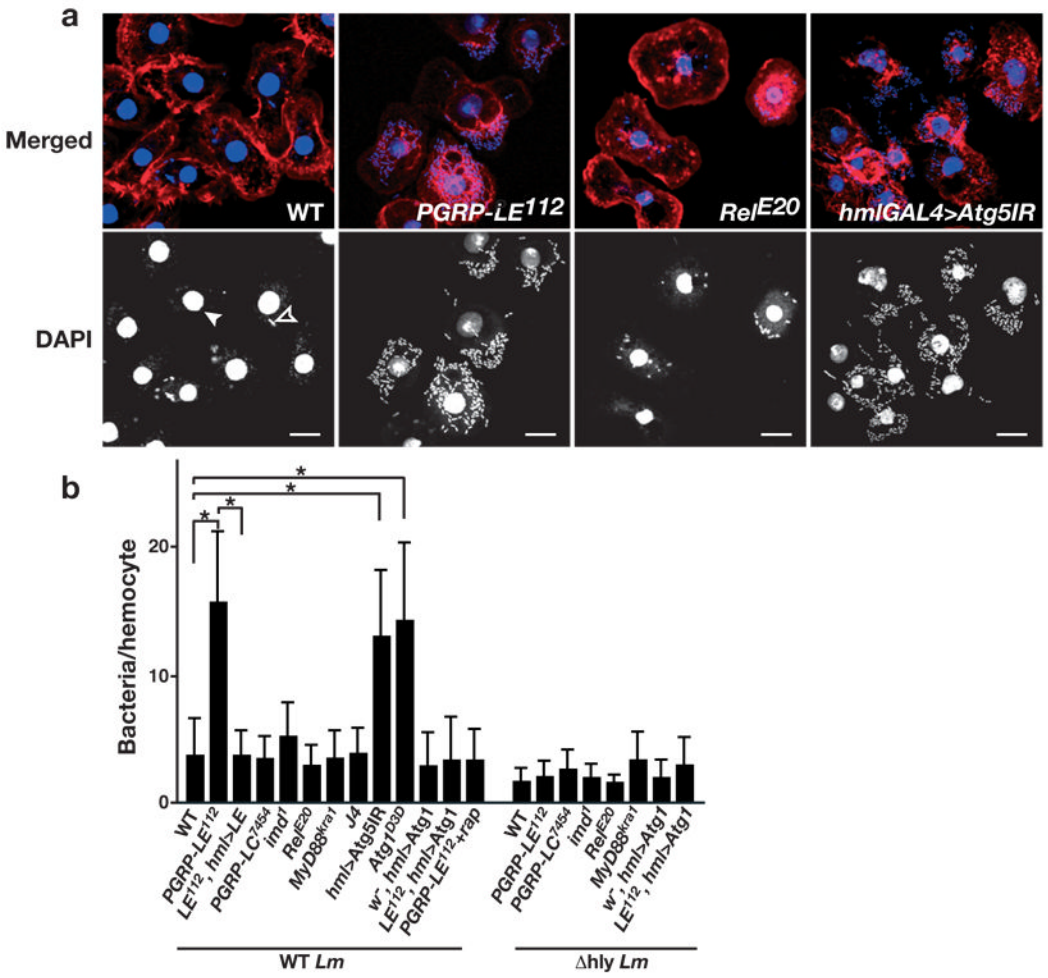

Figure 2.

PGRP-LE and autophagy, but not the Toll and IMD pathways, are required to suppress the intracellular growth of *L. monocytogenes* in hemocytes. (**a**) Hemocytes from third instar larvae of the indicated genotype were cultured *ex vivo* and infected with wild-type *L. monocytogenes*. Hemocyte nuclei (filled arrowhead) and DNA of *L. monocytogenes* (open arrowhead) were visualized by DAPI staining (blue or white), and the actin cytoskeleton was stained with rhodamine-labeled phalloidin (red). For the induction of RNAi against *Atg5*, an inverted repeat sequence of *Atg5* (Atg5IR) was expressed using *hml*-GAL4 (*hml*GAL4>Atg5IR). Bars represent 10 μm. (**b**) The number of intracellular wild-type (WT *Lm*) or Δhly (Δhly *Lm*) *L. monocytogenes* per hemocyte of the indicated genotype was manually counted by DAPI staining of the infected hemocytes. Bars indicate standard deviation of triplicate measurements of at least three independent experiments. *$P < 0.001$ (t-test) each genotype versus wild-type. Genotype abbreviations used: *PGRP-LE*^{112},*ywPGRP-LE*^{112}; *LE*^{112},*hml>LE*, *ywPGRP-LE*^{112}*;UAS-PGRP-LE/+;hml-GAL4/+; PGRP-LC*^{7454}, *w;;PGRP-LC*^{7454}; *Rel*^{E20}, *Relish*^{E20}; J4, Df(2L)J4; *hml>Atg5*IR, *yw*UAS-*Atg5*IR/+;;*hml*-GA4/+; *w*$^{-}$,*hml>Atg1*, *w*$^{-}$*;;UAS-Atg1*^{6B}*/hml-GAL4*, *LE*^{112},*hml>Atg1*, *ywPGRP-LE*^{112}*;;UAS-Atg1*^{6B}*/hml-GAL4*

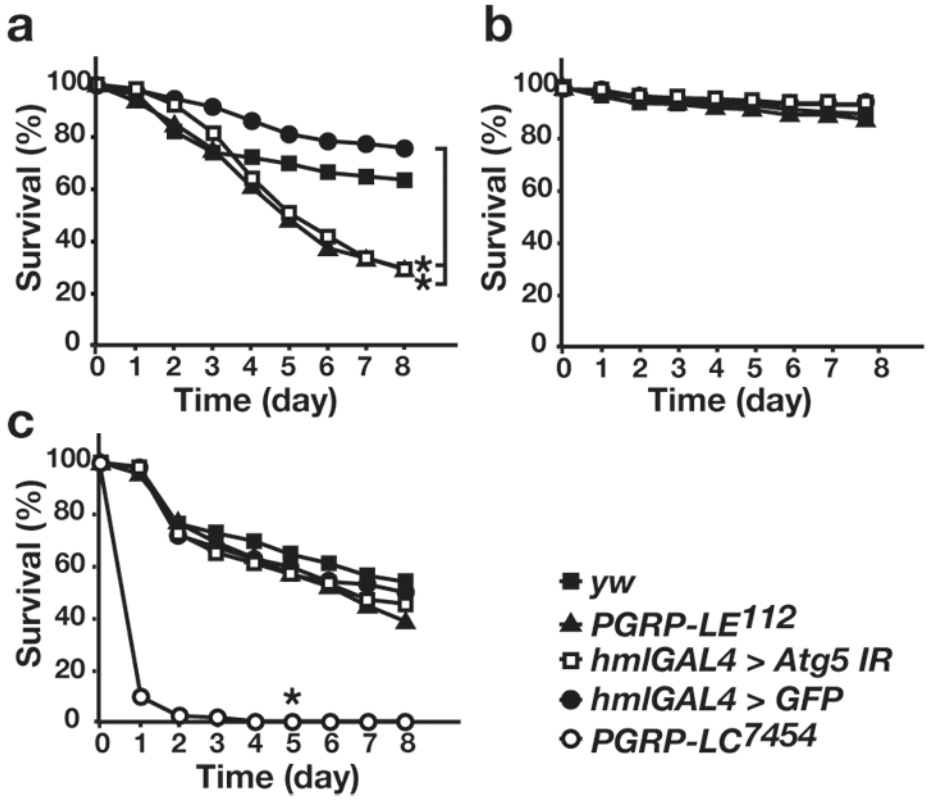

Figure 3.

Autophagy is crucial for host survival against *L. monocytogenes* infection. (**a–c**) Survival rate of *yw* flies, *PGRP-LE*^{112}, *Atg5* RNAi (*hml*-GAL4>*Atg5*IR), and control hml-GAL4-carrying flies (*hml*-GAL4>GFP) after injection of (**a**) wild-type or (**b**) Δ*hly L. monocytogenes*, or (**c**) *E. carotovora* (*Ecc15*) into adult flies. The average survival rate of four independent experiments is shown. * $P < 0.01$ (Wilcoxon-Mann-Whitney test versus hmlGAL4>GFP in (**a**), versus *yw* in (**c**)) (P=0.0024, 0.0007, *hml*-GAL4>GFP versus *hml*-GAL4>*Atg5*IR, *PGRP-LE*^{112}, respectively in (a) P=0.0055, *yw* versus *PGRP-LC*^{7454} flies in (c))

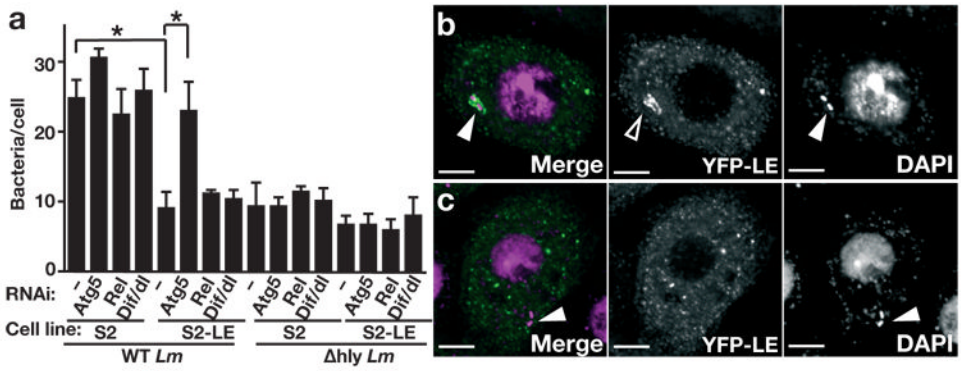

Figure 4.

Autophagy, but not the IMD or Toll pathways, is crucial for PGRP-LE–mediated suppression of intracellular growth of *L. monocytogenes* in S2 cells. (**a**) S2 cells (S2) or S2 cells expressing PGRP-LE (S2-LE) were transfected with double-stranded RNA specific for *Atg5*, *Rel* or *Dif/dl* (RNAi, below graph) and infected with wild-type (WT *Lm*) or Δhly (Δhly *Lm*) *L. monocytogenes* for 1.5 h, followed by 6 h incubation in $CuSO_4$- and gentamicin-containing medium, and *L. monocytogenes* growth was quantified by determining colony-forming units by plate assay. Bars indicate the variance of two independent experiments. **P* < 0.001 (t-test) (**b, c**) Co-localization of PGRP-LE with wild-type *L. monocytogenes* in S2 cells. S2 cells engineered to express YFP-PGRP-LE were infected with (**b**) WT *Lm* or (**c**) Δhly *Lm* for 0.5 h, followed by 1 h incubation in gentamicin-containing medium, DAPI staining, and visualization by fluorescence confocal microscopy. YFP-PGRP-LE (green) and DAPI (magenta) are shown in the merged panel. Closed arrowheads show *L. monocytogenes*, and the open arrowhead indicates YFP-PGRP-LE accumulated around the bacteria. Scale bar, 5 μm.

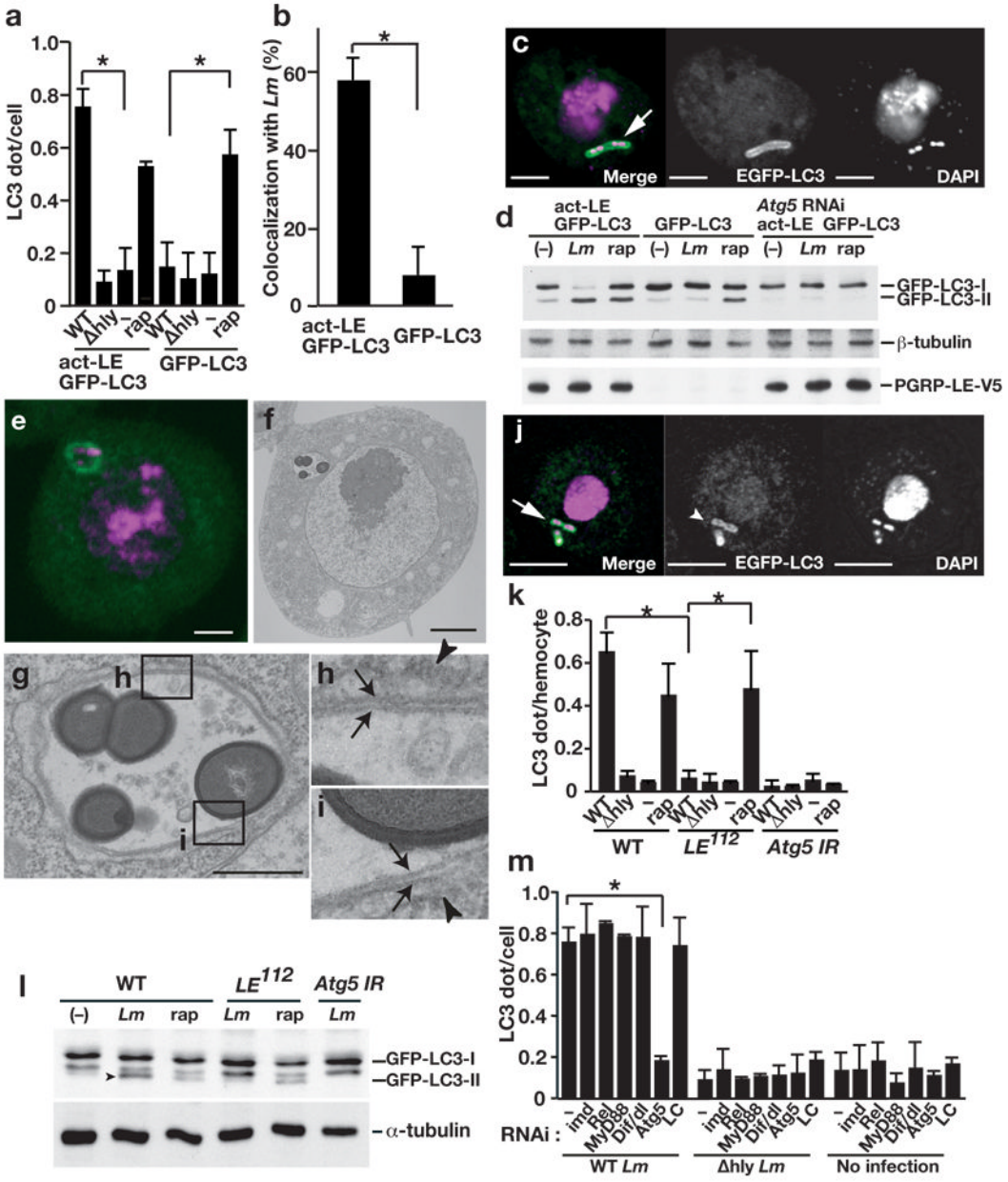

Figure 5.

PGRP-LE mediates autophagosome formation in S2 cells and hemocytes. (**a**) The number of dot- or ring-shaped GFP-LC3 signals per cell was quantified after wild-type (WT) or Δhly *L. monocytogenes* infection or without infection (−) of S2 cells expressing both PGRP-LE and GFP-LC3 or only GFP-LC3, or after 1.5 h incubation with 5 μM rapamycin (rap). Bars indicate standard deviation of triplicate measurements. (**b**) The number of GFP-LC3 dots colocalized with wt *L. monocytogenes* in indicated S2 cells was quantified using confocal microscopy images. Bars indicate standard deviation of triplicate measurements. (**c**) Confocal microscopy images of WT *L. monocytogenes* infected S2 cells expressing PGRP-LE and GFP-LC3. GFP-LC3 (green), DAPI (magenta). Scale bar, 5 μM. Arrow indicates co-localization of GFP-LC3 and *L. monocytogenes*. (**d**) Indicated S2 cells were infected with WT *L. monocytogenes (Lm)*, or treated with 5 μM rapamycin (rap) and indicated proteins in lysates were detected by

immunoblotting. (**e–i**) Ultrastructural analysis of WT *L. monocytogenes*-infected S2 cells expressing PGRP-LE and GFP-LC3. (**e,f**) Fluorescence microscopy (**e**) and electon microscopy (**f**) images of cells expressing GFP-LC3 (green) stained with DAPI (magenta). Scale bars, 1 μm. (**g**) Magnified image of a bacteria-containing vacuole shown in (**f**). Scale bar, 500 nm. (**h, i**) Magnified images of the fields indicated in (**g**). Arrows indicate double-membrane structure that surrounds the bacteria. Arrowheads indicate endoplasmic reticulum–like membrane. (**j**) Confocal microscopy images of WT *L. monocytogenes*-infected hemocytes. GFP-LC3 (green), DAPI (magenta). (**k**) The number of dot- or ring-shaped GFP-LC3 signals per cell in *ex vivo*-cultured hemocytes expressing GFP-LC3 infected or treated as indicated. Bars indicate standard deviation of triplicate measurements. (**l**) Hemocytes from third instar larvae of the indicated genotype were cultured *ex vivo* and infected or treated as indicated and lysates were probed with antibodies specific for the indicated antibodies. Arrowhead indicates processed form of GFP-LC3. (**m**) S2 cells expressing PGRP-LE and GFP-LC3 under the control of an actin promoter were transfected with double-stranded RNA specific for indicated transcripts (RNAi, below graph) and infected with *L. monocytogenes* for 0.5 h. After 1 h incubation in gentamicin-containing medium, GFP-LC3 dot formation was quantified by confocal microscopy. Bars indicate standard deviation of at least triplicate measurements. * $P < 0.001$ (t-test).

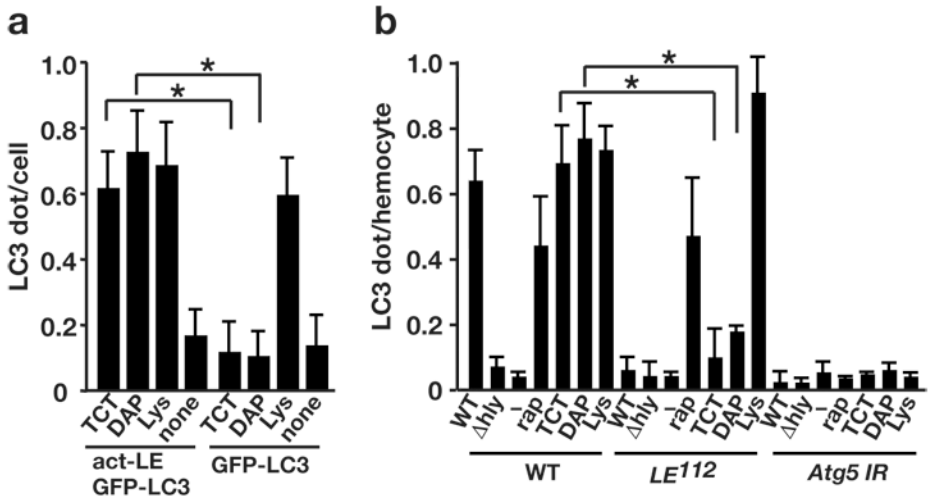

Figure 6.

PGRP-LE is responsible for TCT and DAP-type PGN-induced autophagy. (**a**) S2 cells expressing PGRP-LE (act-LE) and GFP-LC3, or GFP-LC3 only, were treated with 100 nM TCT, 100 μg/ml highly purified DAP-type peptidoglycans from *L. plantarum* (DAP), or lysine-type peptidoglycans from *S. epidermidis* (Lys). After 2 h incubation, GFP-LC3 dot formation was quantified. Bars indicate the variance of two independent experiments. (**b**) The number of dot- or ring-shaped GFP-LC3 signals per hemocyte of indicated genotype was quantified after wild-type (WT) or Δhly *L. monocytogenes* infection, 5 μM rapamycin treatment (rap), or treatment with 100 nM TCT (TCT), 100 μg/ml highly purified DAP-type PGN from *L. plantarum* (DAP), or lysine-type PGN from *S. epidermidis* (Lys). Bars indicate variance of two independent experiments. Genotypes: w^{-}; UAS-GFP-LC3/UAS-Gal4; heat-shock-GAL4/+ (WT), *PGRP-LE*^{112} ; UAS-GFP-LC3/UAS-Gal4; heat-shock-GAL4/+ (*LE*^{112}), UAS-*Atg5* IR/+, UAS-GFP-LC3/UAS-Gal4; heat-shock-GAL4/+ (*Atg5 IR*). * $P < 0.001$ (t-test).